Available online at www.sciencedirect.com
SCIENCE DIRECT®
Bioorganic & Medicinal Chemistry Letters
Bioorganic & Medicinal Chemistry Letters 16 (2006) 461–468

QSAR analysis of meclofenamic acid analogues as selective COX-2 inhibitors

Tamanna Narsinghani[a,*] and S. C. Chaturvedi[b]

[a]*Department of Pharmacy, S.G.S.I.T.S., 23 Park Road, Indore, India*
[b]*School of Pharmacy, DAVV, Takshashila Campus, Khandwa Road, Indore, India*

Received 13 May 2005; revised 8 July 2005; accepted 27 July 2005
Available online 14 November 2005

Abstract—The use of quantitative structure–activity relationships, since its advent, has become increasingly helpful in understanding many aspects of biochemical interactions in drug research. This approach was utilized to explain the relationship of structure with biological activity of selective COX-2 inhibitors. The enormity of the COX-2 discovery is reflected in the unprecedented speed at which research laboratories have sought to validate its clinical implications. Presented herein is a series of 21 derivatives of meclofenamic acid with selective COX-2 inhibitory activity. Several statistically significant regression expressions were obtained for both COX-1 and COX-2 inhibition using sequential multiple linear regression analysis method. Two of these models were selected and validated further, which revealed the importance of Kier molecular flexibility index for COX-2 inhibitory activity and the number of hydrogen bond donor atoms for COX-1 inhibitory activity. Additionally, linear correlation of molecular flexibility with COX-1 and COX-2 inhibitory activities revealed that flexibility of molecules at COX-2 active site can improve the selectivity of COX-2 inhibitors.

Non-steroidal anti-inflammatory drugs (NSAIDs) cause considerable morbidity in terms of dyspepsia, gastrointestinal haemorrhage, renal dysfunction, aggravation of hypertension, and precipitation of heart failure. The gastrointestinal adverse effects are mediated largely through inhibition of Cyclooxygenase-1 (COX-1). This enzyme is also required for the production of thromboxane in platelets and inhibition of thromboxane is purported to reduce the risk of cardiovascular events. Cyclooxygenase-2 (COX-2) mediates not only the analgesic and anti-inflammatory effects of NSAIDs but also the production of prostacyclin in the vascular wall, which may protect against cardiovascular events. COX-2 inhibitors are less likely than COX-1 inhibitors to reduce adverse gastrointestinal effects.[1] Traditional NSAIDs, such as aspirin and indomethacin, inhibit both COX-1 and COX-2. COX-1 is constitutively expressed and produces physiologically important prostaglandins that contribute to mucosal cytoprotection for example. On the other hand, COX-2 is induced significantly under inflammatory conditions. From these facts, the side effects of traditional NSAIDs are believed to be due to the inhibition of COX-1.[2] A large number of research studies aimed at finding selective COX-2 inhibitors have been performed.[3–5] Most of the compounds fit into three main categories: (a) acidic sulfonamides, such as NS-398 and L-745337, and Flosulide, (b) diarylheterocycles, such as Rofecoxib and Celecoxib, and (c) modification of classical NSAIDs, such as zomepirac and indomethacin derivatives (Fig. 1). In the quest for search of selective COX-2 inhibitors, the concept of QSAR was exploited in modifying conventionally available NSAIDs in the hope of developing them as powerful, non-ulcerogenic anti-inflammatory agents.[6,7]

The COX-1 and COX-2 inhibitory activity data of meclofenamic acid analogues were taken from the reported work of Kalgutkar et al.[8] and are presented in Table 1. The title compounds of the present series were shown to exhibit a different mechanism of selectively inhibiting the COX-2 enzyme when compared with diarylheterocycles, and ester and amide derivatives of Indomethacin. The biological activity data

Keywords: COX-1/COX-2/MOE/QSAR/meclofenamic acid analogues.
Abbreviations: COX-1, Cyclooxygenase-1; COX-2, Cyclooxygenase-2; MOE, molecular operating environment; QSAR, quantitative structure–activity relationship.
* Corresponding author. Tel./fax: +91 0731 2546031; e-mail: kashishnarsinghani@rediffmail.com

0960-894X/$ - see front matter © 2005 Published by Elsevier Ltd.
doi:10.1016/j.bmcl.2005.07.067

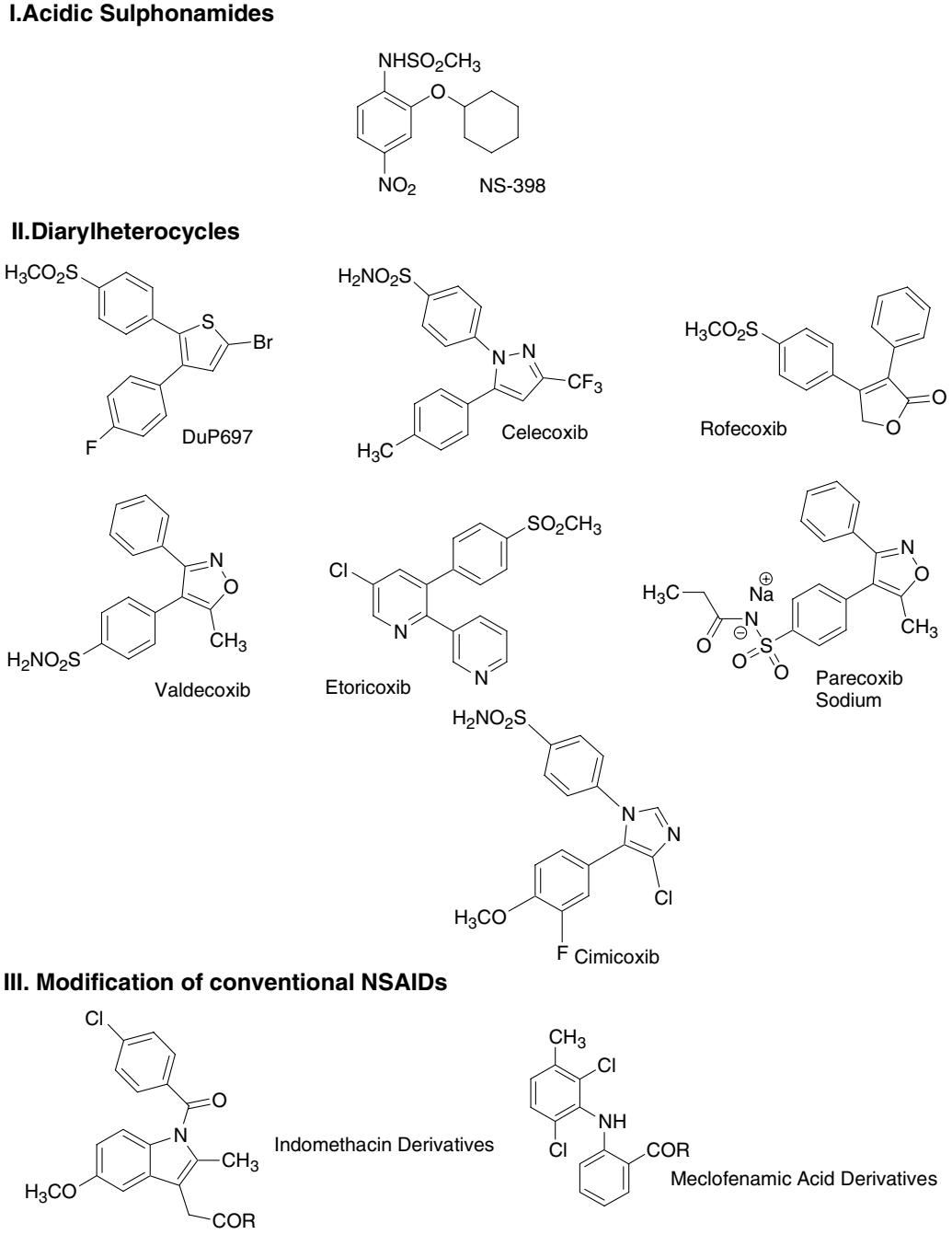

Figure 1. Categories of selective COX-2 inhibitors.

(IC_{50} in micromolar for COX-1 and COX-2 inhibition) were converted to the negative logarithmic dose (pIC_{50}) for a quantitative structure–activity relationship (QSAR) analysis. All the computational work was performed on P-III workstation using Molecular Operating Environment (MOE 2002.03)[9] developed by Chemical Computing Group Inc., Canada, and regression analysis program VALSTAT.[10] The molecular structures of all 21 compounds were sketched using the molecular builder module of software and minimized for energy via steepest descent, conjugate gradient, and truncated Newton method in sequence using MMFF94 as force field with energy tolerance value of root mean square gradient 0.001 kcal/mol and the iteration set limit was set to 1000. A conformational search of each energy-minimized structure was performed using stochastic approach. Stochastic conformational search method is similar to the RIPS method, that generates a new molecular conformation by randomly perturbing the position of each coordinate of each atom in molecule, followed by energy minimization. All conformers generated for each structure were analyzed in conformational geometry panel with great care and the lowest energy conformation of each structure was selected.

The lowest energy conformer of all compounds was transferred to a database viewer to compute various

Table 1. Structures of derivatives of meclofenamic acid, and their COX-1 and COX-2 inhibitory and selectivity data

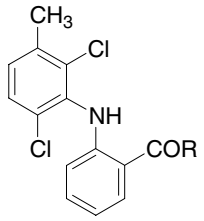

S. No.	Substituent (R)	IC_{50} (μM)[a]		pIC_{50} (μM)[b]		Selectivity[c]	$BA_{(selectivity)}$[d]
		COX-1	COX-2	COX-1	COX-2		
1.	–OH	0.04	0.05	7.398	7.301	0.8	0.097
2.	$-OCH_3$	4.0	17.0	5.398	4.770	0.2	0.699
3.	$-NH(CH_2)_7CH_3$	0.06	0.05	7.222	7.301	1.3	−0.114
4.	$-NH(CH_2)_3Cl$	2.4	0.06	5.619	7.222	40	−1.602
5.	$-NH(CH_2)_2Br$	2.0	0.07	5.699	7.155	28	−1.447
6.	$-NH(CH_2)_2OH$	1.0	0.6	6.000	6.222	1.7	−0.230
7.	$-NH(CH_2)_2OCH_3$	3.0	0.14	5.522	6.854	21	−1.322
8.	$-NH(CH_2)_2OC_6H_5$	66	0.15	4.181	6.824	440	−2.643
9.	$-NH(CH_2)_3OCH_3$	11	0.25	4.959	6.602	44	−1.643
10.	$-NHCOCH_3$	55	0.5	4.259	6.301	110	−2.041
11.	$-NHOC(CH_3)_3$	66	8.0	4.181	5.097	8.0	−0.903
12.	$-NHOCH_2C_6H_5$	66	1.0	4.181	6.000	66	−1.820
13.	$-NHOCH_2C_6H_4NO_2$	66	0.2	4.181	6.699	300	−2.477
14.	$-NHCH_2CH_2C_6H_5$	4.0	4.5	5.398	5.347	0.9	0.046
15.	$-NHNHCH_2C_6H_5$	6.3	5.0	5.201	5.301	1.3	−0.114
16.	$-NHCH_2CO_2CH_3$	1.2	0.07	5.921	7.155	17	−1.230
17	$-NHCH_2CO_2C_2H_5$	4.0	0.2	5.398	6.699	20	−1.301
18.	$-NHCH_2CO_2H$	0.3	0.4	6.523	6.398	0.7	0.155
19.	–NHCH (CH_3) CO_2CH_3 (*S*)	2.6	0.8	5.585	6.097	3.2	−0.505
20.	–NHCH (CH_3) COOH (*S*)	33	6.0	4.482	5.222	5.5	−0.740
21.	–NHCH (CH_3) CO_2CH_3 (*R*)	6.0	2.7	5.222	5.569	3.2	−0.505

[a] IC_{50} (μM) values for inhibition of purified human COX-2 or ovine COX-1.
[b] Negative logarithmic IC_{50} (in moles).
[c] IC_{50} COX-1/IC_{50} COX-2.
[d] Negative logarithmic selectivity.

physicochemical properties utilizing the QuaSAR descriptors module[11] that calculates 193 descriptors partitioned into three classes: 2D-descriptors based on atoms and connection information on molecules, internal i3D-descriptors using three-dimensional coordinate information about each molecule, which are invariant of rotations and translations of the conformation, and external x3D-descriptors that use three-dimensional coordinate information but require an absolute frame of reference. The values of calculated descriptors are given in Table 2.

To establish the correlation between physicochemical parameters as independent variable and COX-1 and COX-2 inhibitory activity as dependent variable, the data were transferred to statistical program VALSTAT. Sequential multiple linear regression analysis method (in sequential multiple regression, the program searches for all permutations and combinations sequentially for the data set) was applied for the same. The best model was selected on the basis of statistical parameters viz., observed squared correlation coefficient (r^2), standard error of estimate (s), and sequential Fischer test (F). Z score (absolute difference between values of model and activity field, divided by the square root of mean square error of data set) was taken as a measure of outlier detection. To assess the self-consistency of derived models, they were validated using leave-one-out (LOO) and the predictive ability was checked using cross-validated squared correlation coefficient (r^2_{cv} or q^2), bootstrapping squared correlation coefficient (r^2_{bs}), chance statistics (evaluated as the ratio of the equivalent regression equations to the total number of randomized sets; a chance value of 0.001 corresponds to 0.1% chance of fortuitous correlation), and outliers (on the basis of Z-score value). The ±data within parentheses are the standard deviation, associated with the coefficient of descriptors in regression equations.

Statistical processing by utilizing the sequential multiple regression analysis method generated several QSAR equations. The quality of a model is reported in statistical terms (e.g., correlation coefficient). The statistically significant parameters are given in Table 3. The best simple linear correlation obtained for COX-1 and COX-2 inhibitions is discussed below.

Table 2. Descriptors calculated for compounds used in derived models for COX-1 and COX-2 inhibition

Compound No.	chi1_C	Kierflex	glob	petitjean	PEOE_VSA_FPPOS	a_don	E_ang	PEOE_VSA + 2	pmiZ	vsa_don
MEC-1	5.877	3.870	0.236	0.500	0.092	3	1.815	8.619	627.166	5.683
MEC-2	5.877	4.393	0.194	0.444	0.050	1	1.456	8.619	458.509	5.683
MEC-3	9.584	8.637	0.089	0.500	0.031	2	2.712	17.238	2562.336	11.365
MEC-4	6.877	6.942	0.157	0.500	0.037	2	2.258	17.238	1012.99	11.365
MEC-5	6.377	6.939	0.177	0.455	0.038	2	1.972	17.238	513.604	11.365
MEC-6	6.377	5.508	0.196	0.455	0.072	3	2.535	17.238	555.598	11.365
MEC-7	6.377	6.098	0.142	0.500	0.037	2	2.129	17.238	554.477	11.365
MEC-8	9.194	6.196	0.266	0.467	0.032	2	3.897	17.238	1311.67	11.365
MEC-9	6.877	6.706	0.144	0.462	0.036	2	2.417	17.238	947.650	11.365
MEC-10	5.877	4.939	0.183	0.500	0.042	2	2.308	8.619	473.555	16.568
MEC-11	7.377	5.635	0.151	0.455	0.035	2	2.586	8.619	613.439	16.568
MEC-12	9.102	5.666	0.222	0.500	0.034	2	2.711	8.619	592.335	16.568
MEC-13	8.918	6.169	0.219	0.500	0.048	2	3.156	8.619	731.637	16.568
MEC-14	9.602	5.666	0.145	0.500	0.034	2	1.979	17.238	482.005	11.365
MEC-15	9.102	5.666	0.076	0.500	0.034	3	3.794	25.857	720.714	15.104
MEC-16	6.285	5.815	0.187	0.500	0.079	2	2.540	17.238	507.791	11.365
MEC-17	6.992	6.393	0.182	0.462	0.075	2	2.937	17.238	902.837	11.365
MEC-18	6.285	5.256	0.177	0.455	0.116	4	2.243	17.238	503.204	11.365
MEC-19	6.788	5.517	0.090	0.500	0.075	2	3.573	3.146	1770.281	11.365
MEC-20	6.788	5.488	0.153	0.455	0.110	4	4.869	17.238	498.987	11.365
MEC-21	7.104	3.835	0.127	0.500	0.083	2	2.999	3.145	278.671	11.365

Table 3. Statistically significant parameters generated for COX-1 and COX-2 inhibition

Model No.	r^2	SE	F	ICAP[a] (upto)	r^2_{bs}	S_{bs}	Chance	q^2	S_{PRESS}	S_{DEP}	No. of outliers
COX-2 inhibition											
1.	0.794	0.406	15.465	0.427	0.840	0.080	0.001	0.605	0.563	0.492	0
2.	0.662	0.521	7.827	0.489	0.725	0.123	0.001	0.411	0.688	0.600	0
COX-1 inhibition											
1.	0.817	0.449	17.913	0.405	0.873	0.084	0.001	0.612	0.655	0.572	0
2.	0.810	0.459	17.032	0.256	0.875	0.075	0.001	0.599	0.666	0.582	0

[a] The maximum limit of intercorrelation among the descriptors used in the generation of equations.

Model No. 1

$$\begin{aligned} \mathrm{pIC}_{50(\mathrm{COX\text{-}2})} &= 0.651(\pm 0.098)\mathrm{kierflex} \\ &\quad - 0.365(\pm 0.082)\mathrm{chi1\_C} \\ &\quad + 9.020(\pm 2.003)\mathrm{glob} \\ &\quad + 21.682(\pm 4.514)\mathrm{petitjean} \\ &\quad - 6.748(\pm 2.280), \\ &\quad n = 21,\ r = 0.891,\ r^2 = 0.794, \\ &\quad \mathrm{SE} = 0.406,\ F = 15.465. \end{aligned}$$

The tetravariant model No. 1 explained 79.4% of the variance in activity. The standard error of estimate of the derived coefficients is less in making a higher t value, hence rendering the terms statistically significant.The observed t values of the descriptors chi1_C (4.45), kierflex (6.64), glob (4.50), and petitjean (4.80) are greater than the tabulated t value (2.12) at 95% confidence interval. The data showed an overall internal statistical significance level better than 99.9%. The dependency among the physicochemical parameters was checked by observing an intercorrelation amongst the parameters (i.e., ICAP). The correlation matrix is given in Table 4. Internal consistency of the models was tested by exploiting leave-one-out and bootstrapping methods of cross-validation. The models were found to be robust having a fairly good predictive ability, as evident from the higher q^2 (0.605), and low S_{PRESS} and S_{DEP} values. The model was tested further for outliers by utilizing the Z score values and no compound was found to be an outlier, which suggested that the model is able to explain the structurally diverse analogues (Table 5, Fig. 2). The r^2_{bs} is at par with the conventional squared correlation coefficient (r^2). Randomization test data (Chance < 0.001) revealed that the results were not based on chance correlation.

Kier molecular flexibility index is given by (KierA1) (KierA2)/n. The Kier and Hall kappa molecular shape indices[12,13] compare the molecular graph with minimal and maximal molecular graphs. The positive contribution of molecular flexibility (kierflex), a topological 2D parameter, indicates the influence of the molecule's shape on COX-2 activity. chi1_C[12,13] is negatively contributing to COX-2 inhibitory activity. Carbon connectivity index (order 1), i.e., chi1_C is calculated as the sum of 1/sqrt($didj$) over all bonds between carbon atoms i and j where $i < j$. Petitjean, a negatively contributing distance and adjacency matrix descriptor is defined as (diameter − radius)/diameter. The largest value in the distance

Table 4. Correlation matrix for the descriptors used in derived models for COX-1 and COX-2 inhibition

	chi1_C	Kierflex	glob	petitjean	PEOE_VSA_FPPOS	a_don	E_ang	PEOE_VSA + 2	pmiZ	vsa_don
chi1_C	1.000									
Kierflex	0.427	1.000								
glob	0.127	0.255	1.000							
petitjean	0.338	0.017	0.241	1.000						
PEOE_VSA _FPPOS	0.509	0.489	0.088	0.218	1.000					
a_don	0.119	0.164	0.043	0.179	0.665	1.000				
E_ang	0.356	0.093	0.182	0.010	0.212	0.405	1.000			
PEOE_VSA + 2	0.217	0.516	0.153	0.174	0.154	0.348	0.131	1.000		
pmiZ	0.409	0.660	0.346	0.206	0.256	0.172	0.233	0.059	1.000	
vsa_don	0.424	0.228	0.115	0.246	0.368	0.001	0.331	0.013	0.043	1.000

Table 5. Calculated pIC_{50} (LOO) with residual and *Z*-score values using model-1 and model-2 for COX-2 inhibition

Compound No.	Model-1			Model-2		
	Calculated (LOO) pIC_{50}	Residual	*Z* score	Calculated (LOO) pIC_{50}	Residual	*Z* score
MEC-1	6.211	1.09	1.938	6.060	1.241	1.713
MEC-2	5.556	−0.786	−1.582	5.044	−0.274	−0.367
MEC-3	6.773	0.528	0.764	7.402	−0.101	−0.113
MEC-4	7.608	−0.386	−0.822	6.964	0.258	0.474
MEC-5	6.834	0.321	0.685	6.214	0.941	1.633
MEC-6	6.134	0.088	−0.211	6.089	0.133	0.249
MEC-7	7.052	−0.198	−0.452	6.291	0.563	1.084
MEC-8	6.184	0.64	1.011	6.911	−0.087	−0.125
MEC-9	6.396	0.206	0.485	5.952	0.65	1.173
MEC-10	6.943	−0.642	−1.416	6.026	0.275	0.498
MEC-11	5.527	−0.43	−0.991	5.398	−0.301	−0.491
MEC-12	6.622	−0.622	−1.276	6.963	−0.963	−1.649
MEC-13	6.870	−0.171	−0.365	7.347	−0.648	−1.120
MEC-14	5.667	−0.32	−0.656	6.179	−0.832	−1.560
MEC-15	5.061	0.24	0.425	5.518	−0.217	−0.324
MEC-16	7.301	−0.146	−0.325	7.080	0.075	0.131
MEC-17	6.501	0.198	0.485	6.680	0.019	0.035
MEC-18	5.758	0.64	1.527	6.279	0.119	0.172
MEC-19	5.999	0.098	0.210	5.955	0.142	0.234
MEC-20	5.658	−0.436	−1.025	6.588	−1.366	−2.035
MEC-21	4.937	0.632	1.172	5.304	0.265	0.388

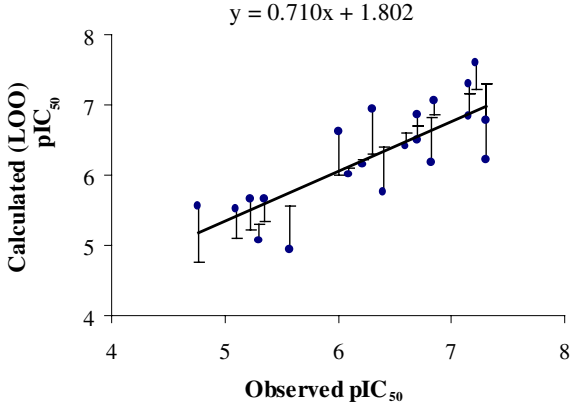

Figure 2. Observed versus calculated (LOO) pIC_{50} for selective COX-2 inhibition using model-1.

matrix is the diameter and the smallest value is the radius. Globularity (a 3D molecular descriptor) is the inverse condition number (smallest eigenvalue divided by the largest eigenvalue) of the covariance matrix of atomic coordinates. A value of 1 indicates a perfect sphere, while a value of 0 indicates a two- or one-dimensional object. This is positively contributing and the value of glob for all the compounds is less than 1, suggesting that the molecules are not perfect spheres but one- or two-dimensional objects that orient themselves at the COX-2 active site, resulting in enzyme inhibition.

Model No. 2

$$\begin{aligned} pIC_{50(COX\text{-}2)} &= 0.613(\pm 0.130)\text{kierflex} \\ &\quad + 9.017(\pm 2.578)\text{glob} \\ &\quad + 12.220(\pm 5.076)\text{PEOE\_VSA\_FPPOS} \\ &\quad + 17.680(\pm 5.568)\text{petitjean} \\ &\quad - 7.115(\pm 2.691), \\ &\quad n = 21,\ r = 0.814,\ r^2 = 0.662, \\ &\quad \text{SE} = 0.521,\ F = 7.827. \end{aligned}$$

Model No. 2 is again a tetravariant model with comparatively lesser r^2 value and q^2 value (Tables 3 and 5,

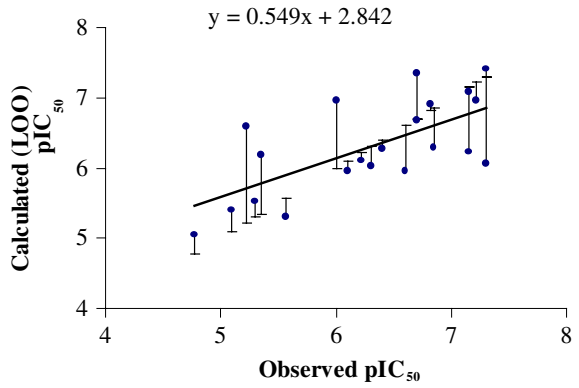

Figure 3. Observed versus calculated (LOO) pIC_{50} for selective COX-2 inhibition using model-2.

Fig. 3). This model explained 66.2% of the variance in activity.

Fractional positive polar van der Waals surface area (PEOE_VSA_FPPOS)[14–16] is the sum of the v_i such that q_i is greater than 0.2 divided by the total surface area. The v_i are calculated using a connection table approximation, which is a partial charge descriptor that utilizes the PEOE method. The partial equalization of orbital electronegativity (PEOE) method of calculating atomic partial charges is a method in which the charge is transferred between bonded atoms until equilibrium. The positive contribution of this parameter reflects the importance of hydrogen bonding of the drug molecule with Tyr355 amino acid residue present in the COX-2 enzyme. This H-bonding may prevent the access of arachidonic acid to the COX-2 enzyme, thereby preventing its conversion into prostaglandins.

Model No. 3

$$\begin{aligned} pIC_{50(COX\text{-}1)} &= 0.749(\pm 0.164)\text{a\_don} \\ &\quad - 0.737(\pm 0.159)\text{E\_ang} \\ &\quad + 0.001(\pm 0.0002)\text{pmiZ} \\ &\quad - 0.132(\pm 0.037)\text{vsa\_don} \\ &\quad + 6.480(\pm 0.572), \\ &\quad n = 21,\ r = 0.904,\ r^2 = 0.817, \\ &\quad \text{SE} = 0.449,\ F = 17.913. \end{aligned}$$

The model No. 3 obtained for COX-1 inhibition is found to explain 81.7% of the variance in activity. It is statistically significant with an F value exceeding 99.9% confidence level. The model is having good predictive ability, which is evident from the obtained q^2 and r^2_{bs} values (Tables 3 and 6, Fig. 4). The low values of S_{PRESS}, S_{DEP}, and S_{bs} also reflect the statistical significance of the model. The independent variables are not highly correlated, as evident from the ICAP value.

a_don is the number of hydrogen bond donor atoms (not counting the basic atoms but counting the atoms that are both hydrogen bond donors and acceptors, such as -OH). It is known that COX-1 selectivity arises because of H-bonding of the carboxylate or amide functionality with the polar Arg120 residue present at the enzyme active site. The positive contribution of a_don proves the same theory. vsa_don represents the approximation to the sum of van der Waals surface areas of pure hydrogen bond donors (not counting the basic atoms and atoms that are both hydrogen

Table 6. Calculated pIC_{50} (LOO) with residual and Z-score values using model-3 and model-4 for COX-1 inhibition

Compound No.	Model-3			Model-4		
	Calculated (LOO) pIC_{50}	Residual	Z-score	Calculated (LOO) pIC_{50}	Residual	Z-score
MEC-1	7.132	0.266	0.419	6.256	1.142	2.074
MEC-2	6.259	−0.861	−1.093	5.695	−0.297	−0.580
MEC-3	6.201	1.021	0.840	6.371	0.851	0.709
MEC-4	5.780	−0.161	−0.369	5.731	−0.112	−0.244
MEC-5	5.490	0.209	0.470	5.383	0.316	0.667
MEC-6	5.868	0.132	0.289	5.797	0.203	0.446
MEC-7	5.425	0.097	0.222	5.283	0.239	0.512
MEC-8	5.071	−0.89	−1.636	4.567	−0.386	−0.714
MEC-9	5.631	−0.672	−1.566	5.532	−0.573	−1.265
MEC-10	4.622	−0.363	−0.699	4.766	−0.507	−1.063
MEC-11	4.533	−0.352	−0.709	4.479	−0.298	−0.615
MEC-12	4.393	−0.212	−0.431	4.291	−0.11	−0.224
MEC-13	4.151	0.03	0.061	4.414	−0.233	−0.488
MEC-14	5.484	−0.086	−0.192	5.270	0.128	0.266
MEC-15	4.491	0.71	1.450	3.946	1.255	1.877
MEC-16	5.012	0.909	2.077	5.933	−0.012	−0.025
MEC-17	5.144	0.254	0.584	5.989	−0.591	−1.292
MEC-18	7.077	−0.554	−0.687	7.516	−0.993	−1.422
MEC-19	5.479	0.106	0.193	5.519	0.066	0.084
MEC-20	5.449	−0.967	−0.938	4.771	−0.289	−0.314
MEC-21	4.376	0.846	1.715	4.288	0.934	1.611

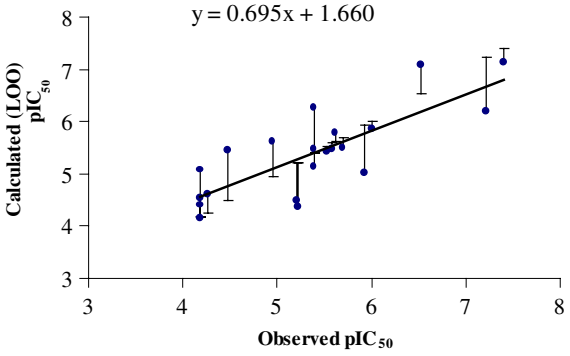

Figure 4. Observed versus calculated (LOO) pIC_{50} for selective COX-1 inhibition using model-3.

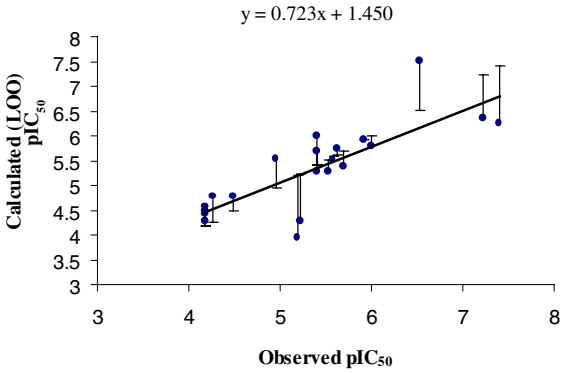

Figure 5. Observed versus calculated (LOO) pIC_{50} for selective COX-1 inhibition using model-4.

bond donors and acceptors, such as -OH). Both a_don and vsa_don are pharmacophore feature descriptors that consider only the heavy atoms in a molecule. E_ang is defined as an angle bend potential energy descriptor and uses the MOE potential energy model to calculate energetic quantities from stored 3D conformations. It is negatively contributing, suggesting that the lowest energy conformer is preferred for binding over the enzyme's active site. Fractional positive polar van der Waals surface area (PEOE_VSA_FPPOS) is positively contributing to COX-1 activity, suggesting that the hydrogen bonding to Tyr355 is important for COX activity. Principal moment of inertia in the z direction (pmiZ) is positively contributing, depicting the effect of symmetry on COX-1 inhibitory activity. The molecule symmetry characteristics are essential for structural configuration of the chemical compound at the specific receptor site.

Model No. 4

$$\begin{aligned} pIC_{50(COX\text{-}1)} &= 0.057(\pm 0.018)\text{PEOE\_VSA} + 2 \\ &\quad - 0.892(\pm 0.140)\text{E\_ang} \\ &\quad + 24.741(\pm 4.148)\text{PEOE\_VSA\_FPPOS} \\ &\quad + 0.001(\pm 0.0002)\text{pmiZ} + 4.677(\pm 0.471), \\ &\quad n = 21,\ r = 0.899,\ r^2 = 0.810, \\ &\quad \text{SE} = 0.459,\ F = 17.032. \end{aligned}$$

The tetravariant model No. 4 was also found to be statistically significant with a comparatively lesser r^2 value. The model was found to have a fairly good predictive ability, as reflected by the cross-validation data (Tables 4 and 6, Fig. 5).

OE_VSA + 2 is positively contributing and it is the sum of v_i where q_i is in the range [0.10, 0.15].

The COX-2 inhibitory activity was found to have a positive correlation with molecular flexibility showing 23.9% variance, as evident from the equation given below.

$$\begin{aligned} pIC_{50(COX\text{-}2)} &= 4.188(\pm 0.876) + 0.364(\pm 0.149)\text{kierflex}, \\ &\quad n = 21,\ r = 0.489,\ r^2 = 0.239, \\ &\quad \text{variance} = 0.515,\ \text{SE} = 0.717,\ F = 5.963. \end{aligned} \quad (1)$$

But when the same independent variable (molecular flexibility) was correlated with COX-1 inhibitory activity, it resulted in the equation shown below, which explained only 0.8% variance of the activity.

$$\begin{aligned} pIC_{50(COX\text{-}1)} &= 4.917(\pm 1.174) + 0.076(\pm 0.200)\text{kierflex}, \\ &\quad n = 21,\ r = 0.089,\ r^2 = 0.008, \\ &\quad \text{variance} = 0.925,\ \text{SE} = 0.962,\ F = 0.146. \end{aligned} \quad (2)$$

This suggests that COX-2 selectivity might arise because of the specific shape of the molecule at the enzyme active site. This specific shape required for COX-2 selectivity cannot be achieved by the same molecules at the COX-1 active site, as is evident from the low value of r^2 in above equation.

When the negative logarithm of selectivity [$IC_{50(COX\text{-}1)}$/$IC_{50(COX\text{-}2)}$] was correlated with the descriptors, similar results were reproduced (Eq. 3).

$$\begin{aligned} BA_{(\text{selectivity})} &= 3.793(\pm 1.214) - 0.269(\pm 0.132)\text{kierflex} \\ &\quad - 10.345(\pm 2.829)\text{glob} \\ &\quad + 0.243(\pm 0.187)\text{adon} \\ &\quad - 0.167(\pm 0.045)\text{vsa\_don}, \\ &\quad n = 21,\ r = 0.820,\ r^2 = 0.673, \\ &\quad \text{SE} = 0.590,\ F = 8.230. \end{aligned} \quad (3)$$

The above equation explains that the descriptors (i.e., kierflex and molecular globularity) are contributing negatively toward the selectivity ratio of IC_{50} of COX-1 against COX-2, suggesting that these descriptors are important for COX-2 selectivity. a_don and vsa_don are contributing positively to selectivity. This reveals that the decrease in the number of hydrogen

bond donor atoms may be responsible for a decrease of $IC_{50(COX\text{-}1)}$ values, which results in the decrease in selectivity.

Thus, the discussed models could be explored further to design potent, non-ulcerogenic anti-inflammatory agents with improved COX-2 selectivity. These models gave an insight into the ways with which COX-2 selectivity could be achieved.

Acknowledgments

Authors are grateful to the Director, Shri G.S. Instt. of Technology and Science, Indore, for providing the facilities for this work and Tata Elxsi, Bangalore, for providing the MOE software. The author T.N. is grateful to AICTE, New Delhi, for providing Junior Research Fellowship.

References and notes

1. Vane, J. *Nature* **1994**, *367*, 215.
2. Cleland, J. G. F. *Lancet* **2002**, *359*, 92.
3. Hashimoto, H.; Imamura, K.; Haruta, J.; Wakitani, K. *J. Med. Chem.* **2002**, *45*, 1511.
4. Reitz, D. B.; Seibert, K. *Annu. Rep. Med. Chem.* **1995**, *30*, 179.
5. Prasit, P.; Riendeau, D. *Annu. Rep. Med. Chem.* **1997**, *32*, 211.
6. Dannhardt, G.; Kiefer, W. *Eur. J. Med. Chem.* **2001**, *36*, 109.
7. Tally, J. J. In *Progress in Medicinal Chemistry*; King, F. D., Oxford, A., Eds.; Elsevier: Amsterdam, 1999; Vol. 36, pp 201–234.
8. Kalgutkar, A. S.; Rowlinson, S. W.; Crews, B. C.; Marnett, L. J. *Bioorg. Med. Chem. Lett.* **2002**, *12*, 521.
9. MOE User's Manual, Tata Elxsi Ltd., Bangalore.
10. Gupta, A. K.; Arockia, B. M.; Kaskhedikar, S. G. *Indian J. Pharm. Sci.* **2004**, *66*(4), 396.
11. Hall, L. H.; Kier, L. B. *Rev. Comput. Chem.* **1991**, *2*.
12. Hall, L. H.; Kier, L. B. *Eur. J. Med. Chem. 12—Chim. Ther.* **1977**, *4*, 307.
13. Wildman, S. A.; Crippen, G. M. *J. Chem. Inf. Comput. Sci.* **1999**, *39*, 868.
14. Lin, A. QuaSAR-descriptor. J. Chem. Compute. Group http://www.chemcomp.com/Journal_of_CCG/Fetures/descr.htm.
15. Labute, P. A. *J. Mol. Graph. Model.* **2000**, *18*, 464.
16. Baurin, N.; Mozziconzcci, J.-C.; Arnoult, E.; Chavette, P.; Marot, C.; Morin-Allory, L. *J. Chem. Inf. Comput. Sci.* **2004**, *44*, 276.